10-7-2015

Relativistic Elastic Differential Cross Sections for Equal Mass Nuclei

Charles M. Werneth
NASA Langley Research Center, Charles.M.Werneth@nasa.gov

Khin M. Maung
University of Southern Mississippi, Khin.Maung@usm.edu

W.P. Ford
University of Southern Mississippi

Physics Letters B 749 (2015) 331–336

Contents lists available at ScienceDirect

Physics Letters B

www.elsevier.com/locate/physletb

Relativistic elastic differential cross sections for equal mass nuclei

C.M. Werneth [a,*], K.M. Maung [b], W.P. Ford [b]

[a] NASA Langley Research Center, 2 West Reid Street, Hampton, VA 23681, United States
[b] The University of Southern Mississippi, 118 College Drive, Box 5046, Hattiesburg, MS 39406, United States

ARTICLE INFO

Article history:
Received 18 November 2014
Received in revised form 29 July 2015
Accepted 2 August 2015
Available online 5 August 2015
Editor: J.-P. Blaizot

Keywords:
Lippmann–Schwinger equation
Relativistic kinematics
Elastic differential cross section

ABSTRACT

The effects of relativistic kinematics are studied for nuclear collisions of equal mass nuclei. It is found that the relativistic and non-relativistic elastic scattering amplitudes are nearly indistinguishable, and, hence, the relativistic and non-relativistic differential cross sections become indistinguishable. These results are explained by analyzing the Lippmann–Schwinger equation with the first order optical potential that was employed in the calculation.

The Lippmann–Schwinger (LS) equation for the transition amplitude is often used to calculate nuclear cross sections for nucleon–nucleus (NA) and nucleus–nucleus (AA) reactions [1]. For the elastic reactions that are considered in the current paper, the LS equation is written as a set of two equivalent equations: the elastic scattering equation and the defining equation for the optical potential. The underlying theory of interaction is motivated by multiple scattering theory (MST), where the sum of nucleon–nucleon (NN) interactions is separated from the unperturbed Hamiltonian of the projectile–target system. The transition amplitude is expressed as a sum of pseudo two-body operators (Watson-τ operators), which are usually approximated by parameterizations of the free NN transition amplitude (impulse approximation). Additionally, single scattering and factorization approximations are used to obtain an optical potential that depends on the NN transition amplitude, nuclear charge densities of the projectile and target, and the initial kinetic energy of the projectile in the laboratory frame [2–5].

There have been several theories that have been used successfully for the prediction of few-body system amplitudes. Three-body systems may be modeled with the Faddeev equations [6–8], and four-body systems may by modeled with the Yakubovsky equations [9]. Furthermore, the Alt–Grassburger–Sandhas (AGS) [10] equations have been used for N-body amplitudes and are found from the $(N-1)$-body and lower amplitudes. Although extremely successful, the Faddeev, Yakubovsky, and AGS equations are limited to few-body problems [11–16].

The model described herein is primarily intended for space radiation applications [4,5], which includes nuclear reactions resulting from collisions of both heavy and light nuclei with projectile kinetic energies extending several orders of magnitude (approximately 10 MeV/n–100 GeV/n) [17,18]. It is for this reason that the MST approach is taken for the NA and AA reactions. The few-body models would not be the best choice for many of reactions that occur in the space radiation environment.

The inclusion of relativity into the LS equation gives rise to interactions which may depend on nuclear spin. However, the impact of relativistic kinematics alone can be significant and — as will be demonstrated — depends on the masses of the projectile and target, projectile energy, and the chosen parameterizations of the transition amplitude and nuclear densities. The non-relativistic (NR) and relativistic (REL) kinematic factors are expressed through the propagator of the AA transition amplitude, and the scattering amplitude is found. Elastic differential cross sections are computed from the absolute square of the scattering amplitude.

In this Letter, the effect of REL kinematics in nucleus–nucleus scattering is studied, and it is found that the scattering amplitudes calculated with REL and NR kinematics are nearly indistinguishable for nuclear collisions of equal mass nuclei when using the first order optical potential. It is shown that there are no observed significant differences between the NR and REL elastic differential cross sections for the equal mass case.

The effects of relativistic kinematics are being studied only in the context of LS equation and the usual assumptions made in the

* Corresponding author.
E-mail address: charles.m.werneth@nasa.gov (C.M. Werneth).

http://dx.doi.org/10.1016/j.physletb.2015.08.002

first order optical potential calculations, such as the impulse approximation, factorization approximation, and neglect of the Fermi motion. We do not imply that this is the only relativistic effect, nor that other effects are unimportant. We are showing that, in the above mentioned context, relativistic kinematic effects are negligible for equal-mass heavy-ion collisions.

The elastic scattering amplitude is determined from the transition amplitude, which is obtained by solving the following integral equation [1],

$$T_{\mathrm{AA}}(\mathbf{k}',\mathbf{k}) = U(\mathbf{k}',\mathbf{k}) + \int \frac{U(\mathbf{k}',\mathbf{k}'')T_{\mathrm{AA}}(\mathbf{k}'',\mathbf{k})}{E_k - E_{k''} + i\epsilon} d\mathbf{k}'', \tag{1}$$

where $\mathbf{k}$ ($\mathbf{k}'$) is the initial (final) relative momentum of the projectile–target system in the center of momentum (CM) frame, E is the NR or REL total energy

$$E_k = \begin{cases} k^2/2\mu & \text{for the NR case,} \\ \sqrt{k^2 + M_{\mathrm{P}}^2} + \sqrt{k^2 + M_{\mathrm{T}}^2} & \text{for the REL case,} \end{cases} \tag{2}$$

M_{P} is the mass of the projectile, M_{T} is the mass of the target, $\mu = (M_{\mathrm{P}}M_{\mathrm{T}})/(M_{\mathrm{P}} + M_{\mathrm{T}})$, and k is the NR or REL relative momentum. $T_{\mathrm{AA}}(\mathbf{k}',\mathbf{k})$ is the off-shell transition amplitude, and $U(\mathbf{k}',\mathbf{k})$ is the optical potential. Using factorization and on-shell approximations for central potentials, the optical potential is expressed as [2–5,19]

$$U(\mathbf{k}',\mathbf{k}) = \eta \mathrm{A_P} \mathrm{A_T} t_{\mathrm{NN}}(|\mathbf{k}' - \mathbf{k}|)\rho_{\mathrm{A_P}}(|\mathbf{k}' - \mathbf{k}|)\rho_{\mathrm{A_T}}(|\mathbf{k}' - \mathbf{k}|), \tag{3}$$

where η is the Möller factor [1,20], $\mathrm{A_P}$ and $\mathrm{A_T}$ are, respectively, the number of nucleons in the projectile and target, t_{NN} is the nucleon–nucleon (NN) transition amplitude, and $\rho(|\mathbf{k}' - \mathbf{k}|)$ is the nuclear density of a nucleus [21,22]. For equal mass projectile and target nuclei ($\mathrm{A_P} = \mathrm{A_T} = \mathrm{A}$), $\eta = 1$, and the optical potential is

$$U(\mathbf{k}',\mathbf{k}) = \mathrm{A}^2 \rho_{\mathrm{A}}^2(|\mathbf{k}' - \mathbf{k}|) t_{\mathrm{NN}}(|\mathbf{k}' - \mathbf{k}|). \tag{4}$$

The on-shell scattering amplitude is related to the on-shell transition amplitude by [1]

$$f(k,k,\hat{\mathbf{k}}\cdot\hat{\mathbf{k}}') = -(2\pi)^2 k \frac{dk}{dE_k} t(k,k,\hat{\mathbf{k}}'\cdot\hat{\mathbf{k}}). \tag{5}$$

The off-shell scattering amplitude is defined as

$$f(\mathbf{k}',\mathbf{k}) \equiv \beta(k')\ \langle \mathbf{k}'|t(E(k'') + i\epsilon)|\mathbf{k}\rangle\ \beta(k), \tag{6}$$

where $\mathbf{k}' \neq \mathbf{k}'' \neq \mathbf{k}$, and

$$\beta(k) = 2\pi i \sqrt{k \frac{dk}{dE_k}}, \tag{7}$$

such that equation (5) is satisfied when the relative momentum is on-shell.

The relative momentum can be expressed as

$$k = \begin{cases} \sqrt{\frac{2\mu M_{\mathrm{T}} T_{\mathrm{Lab}}}{M_{\mathrm{P}} + M_{\mathrm{T}}}} & \text{for the NR case,} \\ \frac{M_{\mathrm{T}}}{\sqrt{s}} \sqrt{T_{\mathrm{Lab}}(T_{\mathrm{Lab}} + 2M_{\mathrm{P}})} & \text{for the REL case,} \end{cases} \tag{8}$$

where μ is the reduced mass, T_{Lab} is the kinetic energy of the projectile in the laboratory frame, and $s = (M_{\mathrm{P}} + M_{\mathrm{T}})^2 + 2M_{\mathrm{T}}T_{\mathrm{Lab}}$ is the Mandelstam variable. In the equal mass limit, $M_{\mathrm{P}} = M_{\mathrm{T}} = M$, the relative momentum reduces to $k = k_{\mathrm{NR}} = k_{\mathrm{REL}} = \sqrt{\frac{MT_{\mathrm{Lab}}}{2}}$.

In order to show that the NR and REL elastic differential cross sections are the same for equal mass systems, the off-shell scattering amplitudes are obtained by using equation (6);

$$\begin{aligned} &\beta_{\mathrm{AA}}(k')T_{\mathrm{AA}}(\mathbf{k}',\mathbf{k})\beta_{\mathrm{AA}}(k) \\ &= \frac{\beta_{\mathrm{AA}}(k')}{\beta_{\mathrm{NN}}(\kappa')}\beta_{\mathrm{NN}}(\kappa')t_{\mathrm{NN}}(|\mathbf{k}' - \mathbf{k}|)\beta_{\mathrm{NN}}(\kappa)\frac{\beta_{\mathrm{AA}}(k)}{\beta_{\mathrm{NN}}(\kappa)} A^2 \rho_A^2(|\mathbf{k}' - \mathbf{k}|) \\ &\quad + \mathbf{P}\int \Bigg[\beta_{\mathrm{AA}}(k')\frac{\beta_{\mathrm{NN}}(\kappa')}{\beta_{\mathrm{NN}}(\kappa')} t_{\mathrm{NN}}(|\mathbf{k}' - \mathbf{k}''|)\frac{\beta_{\mathrm{NN}}(\kappa'')}{\beta_{\mathrm{NN}}(\kappa'')} \\ &\quad \times A^2 \rho_A^2(|\mathbf{k}' - \mathbf{k}''|) \\ &\quad \times \frac{1}{E_k - E_{k''}} \frac{\beta_{\mathrm{AA}}(k'')}{\beta_{\mathrm{AA}}(k'')} T_{\mathrm{AA}}(|\mathbf{k}'' - \mathbf{k}|)\beta_{\mathrm{AA}}(k) d\mathbf{k}'' \Bigg] \\ &\quad - i\pi \int \Bigg[\beta_{\mathrm{AA}}(k')\frac{\beta_{\mathrm{NN}}(\kappa')}{\beta_{\mathrm{NN}}(\kappa')} t_{\mathrm{NN}}(|\mathbf{k}' - \mathbf{k}|)\frac{\beta_{\mathrm{NN}}(\kappa'')}{\beta_{\mathrm{NN}}(\kappa'')} \\ &\quad \times A^2 \rho_A^2(|\mathbf{k}' - \mathbf{k}''|) \\ &\quad \times \delta\Big(E_k - E_{k''}\Big)\frac{\beta_{\mathrm{AA}}(k'')}{\beta_{\mathrm{AA}}(k'')} T_{\mathrm{AA}}(\mathbf{k}'',\mathbf{k})\beta_{\mathrm{AA}}(k) d\mathbf{k}'' \Bigg], \end{aligned} \tag{9}$$

where

$$\beta_{\mathrm{AA}}^2 = \begin{cases} -(2\pi)^2 \frac{\mathrm{A}m}{2} & \text{for the NR case,} \\ -(2\pi)^2 \mathrm{A} \frac{\sqrt{m^2 + \kappa^2}}{2} & \text{for the REL case,} \end{cases} \tag{10}$$

$$\beta_{\mathrm{NN}}^2 = \begin{cases} -(2\pi)^2 \frac{m}{2} & \text{for the NR case,} \\ -(2\pi)^2 \frac{\sqrt{m^2 + \kappa^2}}{2} & \text{for the REL case,} \end{cases} \tag{11}$$

and the propagator has been expressed in terms of its principal value, $\mathbf{P}$,

$$\frac{1}{E_k - E_{k''} + i\eta} = \mathbf{P}\left(\frac{1}{E_k - E_{k''}}\right) - i\pi\delta(E_k - E_{k''}). \tag{12}$$

The Fermi motion of the nucleons inside the nucleus is neglected; therefore, the momentum imparted to each nucleon is $\kappa = k/\mathrm{A}$. The mass of the nucleus, M, is approximately $\mathrm{A}m$, where m is the average nucleon mass.

The pole structure for NR scattering amplitude is proportional to $1/(k^2 - k''^2)$. With REL kinematics, the propagator can be rationalized such that the pole structure is manifestly the same as the NR case, thus

$$\begin{aligned} &\mathbf{P}\left(\frac{1}{E_k - E_{k''}}\right) \\ &= \begin{cases} \mathbf{P}\left[\frac{2\mu}{(k^2 - k''^2)}\right] & \text{for the NR case} \\ \mathbf{P}\left[\left(\frac{\sqrt{M^2 + k^2}}{2}\right)\left(\frac{1 + \sqrt{\frac{M^2 + k''^2}{M^2 + k^2}}}{k^2 - k''^2}\right)\right] & \text{for the REL case,} \end{cases} \end{aligned} \tag{13}$$

where $\mu = \mathrm{M}/2$.

Using equations (10), (11), and (13), the scattering amplitude from equation (9) reduces to the following for on-shell scattering:

$$\begin{aligned} F_{\mathrm{AA}}(k,\hat{\mathbf{k}}'\cdot\hat{\mathbf{k}}) &= f_{\mathrm{NN}}(k,\hat{\mathbf{k}}'\cdot\hat{\mathbf{k}})\mathrm{A}^3\rho_A(k,\hat{\mathbf{k}}'\cdot\hat{\mathbf{k}}) \\ &\quad + \mathbf{P}\int \frac{f_{\mathrm{NN}}(|\mathbf{k}' - \mathbf{k}''|)h(k,k'')\mathrm{A}^3\rho_{\mathrm{A}}^2(|\mathbf{k}' - \mathbf{k}''|)F_{\mathrm{AA}}(|\mathbf{k}'' - \mathbf{k}|)}{[-(2\pi)^2](k^2 - k''^2)} d\mathbf{k}'' \\ &\quad - i\pi \int f_{\mathrm{NN}}(k,\hat{\mathbf{k}}'\cdot\hat{\mathbf{k}}'')\mathrm{A}^3\rho_{\mathrm{A}}^2(k,\hat{\mathbf{k}}'\cdot\hat{\mathbf{k}}'') \\ &\quad \times F_{\mathrm{AA}}(k,\hat{\mathbf{k}}''\cdot\hat{\mathbf{k}})\frac{k}{-(2\pi)^2} d\Omega_{k''} \end{aligned} \tag{14}$$

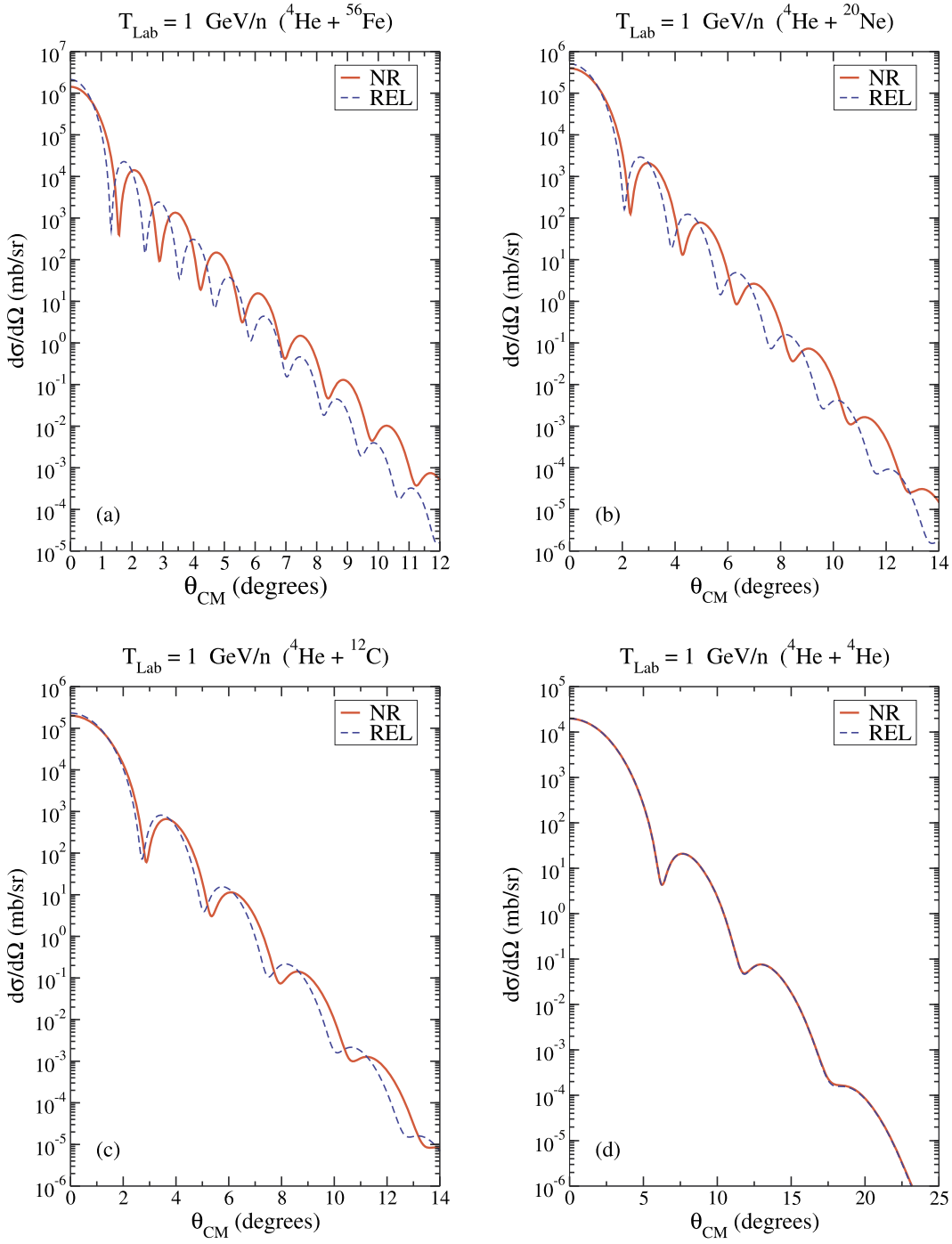

Fig. 1. Elastic differential cross sections for ^{4}He + ^{56}Fe, ^{4}He + ^{20}Ne, ^{4}He + ^{12}C, and ^{4}He + ^{4}He reactions at a lab projectile energy of 1 GeV/n. NR results are indicated with solid red lines, and REL results are given as dashed blue lines. (For interpretation of the references to color in this figure legend, the reader is referred to the web version of this article.)

where

$$\begin{cases} h(k,k'') = 2 & \text{for the NR case} \\ h(k,k'') = 1 + \sqrt{\frac{M^2+k''^2}{M^2+k^2}} & \text{for the REL case.} \end{cases} \tag{15}$$

The only difference between the two amplitudes is that $h(k,k'') = 2$ in the NR case, and $h(k,k'') \to 2$ only near the elastic cut for the REL case. The optical potential is largest near the on-shell momentum but decays rapidly thereafter. By definition, the principal value integral is never evaluated at $k'' = k$; however, significant contributions occur *near* the elastic cut. Due to the rapidly decaying optical potential and large contributions near the elastic cut, little differences are observed between the NR and REL scattering amplitudes for projectiles and targets of equal mass.

The above derivation shows that when $M_P = M_T = M$, the REL and NR scattering amplitudes are approximately equal, therefore $|\psi^{(+)_{REL}}\rangle \approx |\psi^{(+)_{NR}}\rangle$. This approximation allows for a convenient summary of our calculation. The relativistic and non-relativistic half off-shell transition amplitudes can be related by

$$\begin{aligned} T_{NR}(\boldsymbol{k}', \boldsymbol{k}) &= \langle \boldsymbol{k}' | T_{NR} | \boldsymbol{k} \rangle = \langle \boldsymbol{k}' | U_{NR} | \psi_{\boldsymbol{k}}^{(+)} \rangle \\ &= \langle \boldsymbol{k}' | G_{NR}^{-1} | \psi_{\boldsymbol{k}}^{(+)} \rangle = \langle \boldsymbol{k}' | G_{NR}^{-1} G_{REL} G_{REL}^{-1} | \psi_{\boldsymbol{k}}^{(+)} \rangle \end{aligned}$$

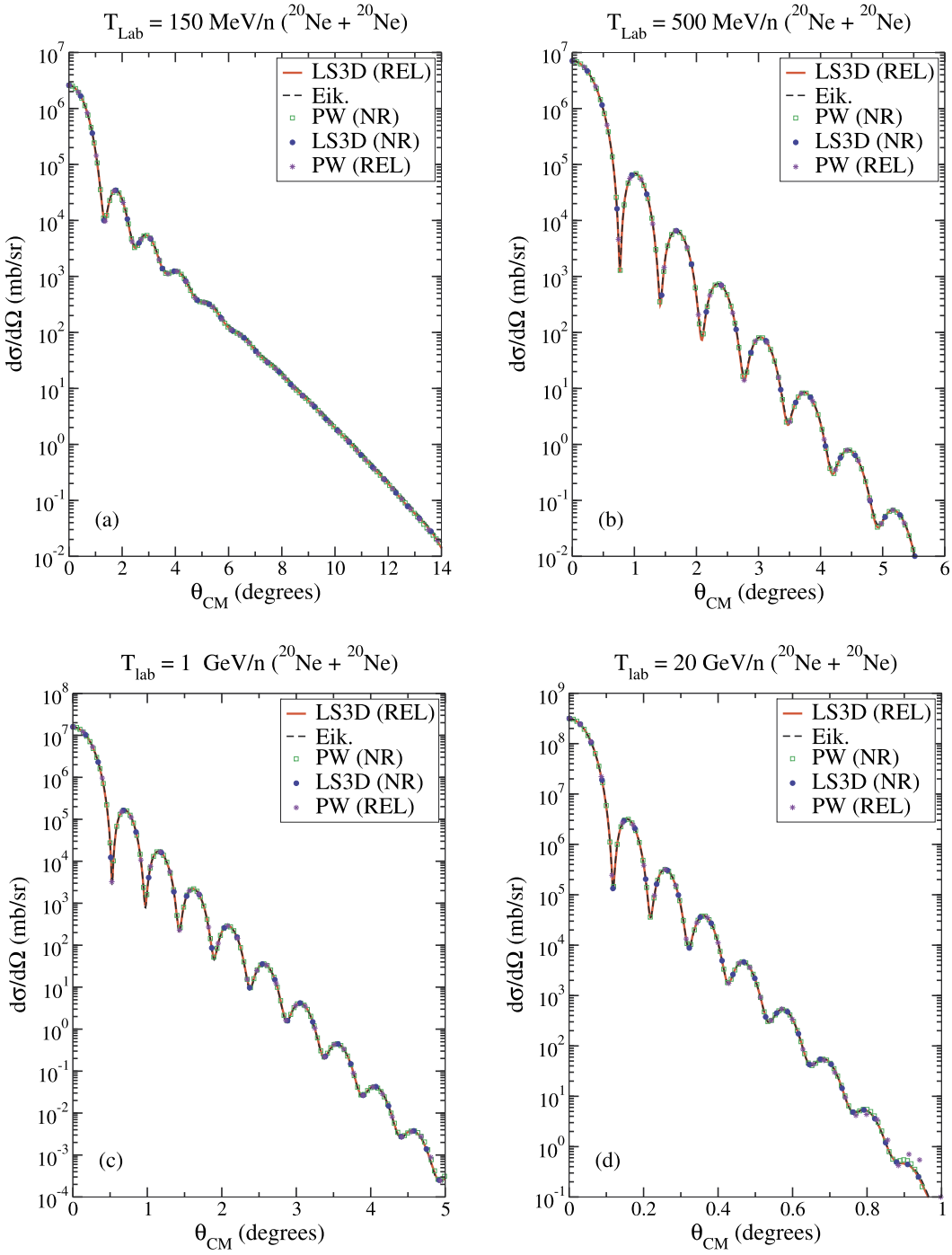

Fig. 2. Elastic differential cross sections for ^{20}Ne + ^{20}Ne reactions for projectile lab kinetic energies of 150, 500, 1000, 20 000 MeV/*n*. Eik. represents eikonal, LS3D represents three-dimensional Lippmann–Schwinger, and PW represents partial wave. Non-relativistic results are denoted (NR) and relativistic results are denoted (REL).

$$
\begin{aligned}
&= \langle \boldsymbol{k}' | G_{\mathrm{NR}}^{-1} G_{\mathrm{REL}} U_{\mathrm{REL}} | \psi_{\boldsymbol{k}}^{(+)} \rangle \\
&= \frac{k^2 - k'^2}{2\mu[E(k) - E(k')]} \langle \boldsymbol{k}' | U_{\mathrm{REL}} | \psi_{\boldsymbol{k}}^{(+)} \rangle \\
&= \xi T_{\mathrm{REL}}(\boldsymbol{k}', \boldsymbol{k}) \qquad (16)
\end{aligned}
$$

where the propagators in momentum space are

$$G_{\mathrm{NR}} = \frac{2\mu}{k^2 - k'^2 + i\epsilon}, \qquad (17)$$

$$G_{\mathrm{REL}} = \frac{1}{E(k) - E(k') + i\epsilon}, \qquad (18)$$

$$E(k) = 2\sqrt{M^2 + k^2}, \qquad (19)$$

and

$$\xi = \frac{k^2 - k'^2}{2\mu[E(k) - E(k')]}, \qquad (20)$$

where

$$\lim_{k' \to k} \xi = \frac{E(k)}{4\mu}. \qquad (21)$$

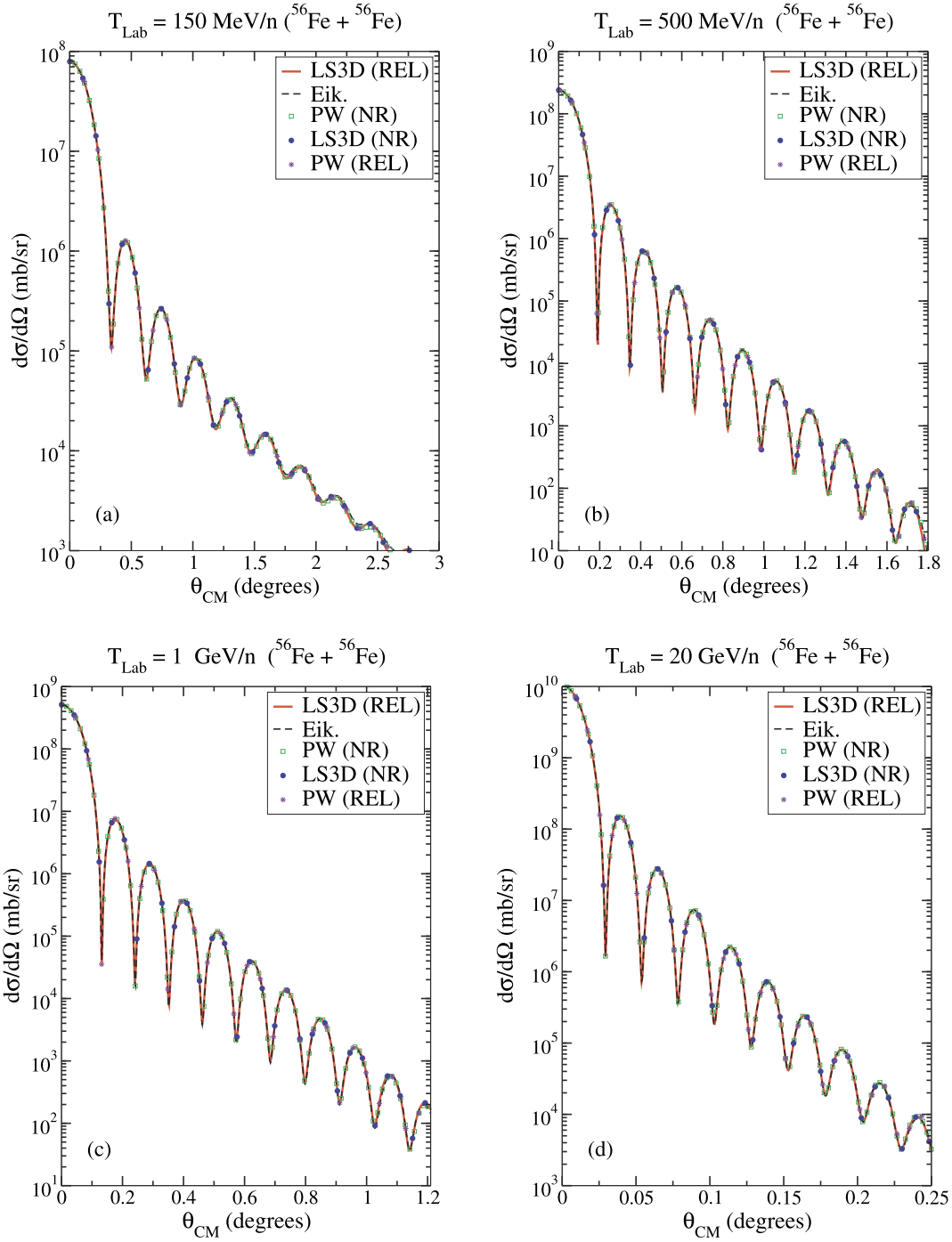

Fig. 3. Elastic differential cross sections for ^{56}Fe + ^{56}Fe reactions for projectile lab kinetic energies of 150, 500, 1000, 20 000 MeV/*n*. Eik. represents eikonal, LS3D represents three-dimensional Lippmann–Schwinger, and PW represents partial wave. Non-relativistic results are denoted (NR) and relativistic results are denoted (REL).

Examining this result for the scattering amplitude in the on-shell limit

$$F_{\mathrm{NR}}(k,\boldsymbol{k}\cdot\boldsymbol{k}') = -(2\pi)^2 k \left.\frac{dk}{dE}\right|_{\mathrm{NR}} T_{\mathrm{NR}}(k,\boldsymbol{k}\cdot\boldsymbol{k}') = -(2\pi)^2 \mu T_{\mathrm{NR}}(k,\boldsymbol{k}\cdot\boldsymbol{k}') \tag{22}$$

$$F_{\mathrm{REL}}(k,\boldsymbol{k}\cdot\boldsymbol{k}') = -(2\pi)^2 k \left.\frac{dk}{dE}\right|_{\mathrm{REL}} T_{\mathrm{REL}}(k,\boldsymbol{k}\cdot\boldsymbol{k}') = -(2\pi)^2 \mu_{\mathrm{REL}} T_{\mathrm{REL}}(k,\boldsymbol{k}\cdot\boldsymbol{k}') \tag{23}$$

where $\mu_{\mathrm{REL}} = \frac{E_P E_T}{E_P + E_T} = \frac{E(k)}{4}$. We can then write

$$F_{\mathrm{REL}}(k,\boldsymbol{k}\cdot\boldsymbol{k}') = -(2\pi)^2 \frac{\mu_{\mathrm{REL}}}{\xi} T_{\mathrm{NR}}(k,\boldsymbol{k}\cdot\boldsymbol{k}') = -(2\pi)^2 T_{\mathrm{NR}}(k,\boldsymbol{k}\cdot\boldsymbol{k}'), \tag{24}$$

$$F_{\mathrm{REL}}(k,\boldsymbol{k}\cdot\boldsymbol{k}') = F_{\mathrm{NR}}(k,\boldsymbol{k}\cdot\boldsymbol{k}'), \tag{25}$$

which is a valid approximation for nucleus–nucleus scattering when $M_{\mathrm{P}} = M_{\mathrm{T}}$.

There are many uncertainties that have been considered when selecting the fundamental parameterizations of transition amplitude in the results that follow. Recently, Okorokov [23] has compiled slope parameter data from various experiments. Often exper-

imentalists use amplitudes that are similar to the form used in the current work, but, in many cases, more than one parameter is varied to obtain a good fit to experimental data. For example, when one attempts to extract the real to imaginary ratio from experimental data, there are different approaches that may be used. The real to imaginary ratio of the transition amplitude, α, is usually extracted at $-|t| = 0$. In order to extract α from measurements of the differential cross section, the total cross section must be known. Experimentalists do not consistently use a single method for evaluating the total cross NN cross section. In some cases the total cross section is taken from other experiments at similar energy for the same reaction, and, for other cases, the total cross section is treated as a parameter such that overall transition amplitude gives the best fit to experimental data. Thus, adjustments to the relative momentum due to kinematic considerations in the data would have been compensated by variation in other parameters of the transition amplitude. The lack of spin-dependent models for use in extraction of the transition amplitude parameters further compounds the issue of uncertainty. It was also found that Coulomb and nuclear-Coulomb interference was not always taken into account [24]. Moreover, there is a dearth of data in general for proton–neutron reactions [25] which also contributes to uncertainty. Given the uncertainty associated the knowledge of the fundamental parameters, the approach taken in the current work and in a previous studies [4,26] — where model results are in good agreement with data — appears to be reasonable.

To illustrate these results, elastic differential cross sections are given in Fig. 1 for ^{4}He + ^{56}Fe, ^{4}He + ^{20}Ne, ^{4}He + ^{12}C, and ^{4}He + ^{4}He reactions at a lab projectile energy of 1 GeV/n. NR and REL elastic differential cross sections are generated with a three-dimensional Lippmann–Schwinger (LS3D) solution [27–30]. See Ref. [5] for the explicit form of the nuclear densities, transition amplitude, and parameterizations that were used in the current work.

From Fig. 1, it is obvious that the NR and REL elastic differential cross sections are different for the ^{4}He + ^{56}Fe, ^{4}He + ^{20}Ne, and ^{4}He + ^{12}C reactions, where the projectile and target masses differ. It is also observed that the largest REL difference occurs in the case of ^{4}He + ^{56}Fe, where the mass difference between the projectile and target is largest. There are no significant differences between the NR and REL results for the equal mass case of the ^{4}He + ^{4}He reaction.

Next, eikonal (Eik), partial wave (PW), and LS3D codes are used to predict the elastic differential cross sections for ^{20}Ne + ^{20}Ne reactions in Fig. 2 and ^{56}Fe + ^{56}Fe reactions in Fig. 3 with lab projectile kinetic energies of 150, 500, 1000, and 20 000 MeV/n. These solution methods are fully described in Refs. [1–3,5,19,27–30]. The PW and LS3D results are generated with NR and REL kinematics, whereas the Eik code is NR. Each figure shows that there is no significant difference between the NR and REL elastic differential cross sections, regardless of the energy.

In summary, it is noted that the REL propagator has pole structure that is similar to the NR case and that the REL and NR scattering amplitudes are approximately equal near the elastic cut. The optical potential is largest near the on-shell momentum and decays rapidly thereafter. Consequently, the NR and REL on-shell scattering amplitudes have been shown to be nearly indistinguishable for projectile and target nuclei of equal mass.

Acknowledgements

The authors would like to thank Drs. John Norbury, Steve Blattnig, Ryan Norman, Jonathan Ransom, and Francis Badavi for reviewing this manuscript. The authors also thank the referees for their helpful comments. This work was supported by the Human Research Program under the Human Exploration and Operations Mission Directorate of NASA and NASA grant number NNX13AH31A.

References

[1] C.J. Joachain, Quantum Collision Theory, American Elsevier, New York, 1983.
[2] A. Picklesimer, P.C. Tandy, R. Thaler, D. Wolfe, Phys. Rev. C 30 (1984) 1861.
[3] A. Picklesimer, P.C. Tandy, R. Thaler, D. Wolfe, Phys. Rev. C 29 (1984) 1582.
[4] C.M. Werneth, et al., Phys. Rev. C 90 (2014) 064905.
[5] C.M. Werneth, et al., Elastic Differential Cross Sections, NASA Technical Publication 2014-218529.
[6] L.D. Faddeev, Sov. Phys. JETP 12 (1961) 1014.
[7] L.D. Faddeev, Mathematical Aspects of the Three Body Problem in Quantum Scattering Theory, Davey, New York, 1965.
[8] L.D. Faddeev, S.P. Merkuriev, Quantum Scattering Theory for Several Particle Systems, Kluwer Academic Publishers, Dordrecht, 1993.
[9] O.A. Yakubovsky, Sov. J. Nucl. Phys. 5 (1967) 937.
[10] E.O. Alt, P. Grassberger, W. Sandhas, Phys. Rev. C 1 (1970) 85.
[11] A. Deltuva, A.C. Fonseca, Phys. Rev. C 76 (2007) 021001.
[12] A. Deltuva, et al., Phys. Rev. C 76 (2007) 064602.
[13] A. Deltuva, Phys. Rev. C 79 (2009) 021602.
[14] A. Deltuva, Phys. Rev. C 79 (2009) 054603.
[15] A. Deltuva, Phys. Rev. C 80 (2009) 064002.
[16] M. Viviani, et al., Phys. Rev. C 84 (2011) 054010.
[17] E.R. Benton, E.V. Benton, Nucl. Instrum. Methods Phys. Res., Sect. B, Beam Interact. Mater. Atoms 184 (2001) 255.
[18] M. Durante, F.A. Cucinotta, Rev. Mod. Phys. 83 (2011) 1245.
[19] D.H. Wolfe, Ph.D. thesis, Kent State University, 1983.
[20] C. Möller, K. Dan. Vidensk. Selsk. Mat.-Fys. Medd. 23 (1945) 1.
[21] C.W. De Jager, H. De Vries, C. De Vries, At. Data Nucl. Data Tables 14 (1974) 479.
[22] H. De Vries, C.W. De Jager, C. De Vries, At. Data Nucl. Data Tables 36 (1987) 495.
[23] V.A. Okorokov, Adv. High Energy Phys. 2015 (2015) Article ID 914170, http://dx.doi.org/10.1155/2015/914170.
[24] T. Lasinski, R.L. Setti, B. Schwartzchild, P. Ukleja, Nucl. Phys. B 37 (1972) 1.
[25] K. Olive, et al., Chin. Phys. C 38 (2014) 090001.
[26] C.M. Werneth, K.M. Maung, L.R. Mead, S.R. Blattnig, Nucl. Instrum. Methods Phys. Res., Sect. B, Beam Interact. Mater. Atoms 308 (2013) 40.
[27] Ch. Elster, J.H. Thomas, W. Glöckle, arXiv:nucl-th/9708017v1, 1997.
[28] I. Fachruddin, Ch. Elster, W. Glöckle, Phys. Rev. C 62 (2000) 044002.
[29] M. Rodriguez-Gallardo, et al., Phys. Rev. C 78 (2008) 034602.
[30] S. Veerasamy, Ch. Elster, W.N. Polyzou, Few-Body Syst. 54 (2013) 2207.